Radiation Physics and Chemistry 182 (2021) 109365

Contents lists available at ScienceDirect

Radiation Physics and Chemistry

journal homepage: www.elsevier.com/locate/radphyschem

Study on attenuation of 3D printing commercial filaments on standard X-ray beams for dosimetry and tissue equivalence

M. Savi [a,b,*], D. Villani [a], M.A.B. Andrade [b], O. Rodrigues Jr. [a], M.P.A. Potiens [a]

[a] Instituto de Pesquisas Energéticas e Nucleares – IPEN. Avenida Lineu Prestes, 2242 Cidade Universitária, 05508-000, São Paulo – SP, Brazil
[b] Instituto Federal de Santa Catarina – IFSC. Avenida Mauro Ramos, 950. Centro, 88020-300, Florianópolis, SC, Brazil

ARTICLE INFO

Keywords:
3D printing
Photon beams
Attenuation coefficients

ABSTRACT

3D printing techniques and materials have become widely available in the last couple of decades and remains an important topic of research as the equipments and supplements gets chipper. This study aims to evaluate the attenuation behaviour of several commercially available 3D printing filaments (ABS and PLA-based filaments and other polymers blends) over standard X-ray beams ranging from ~30 keV - to ~50 keV and comparing the experimental results with theoretical data of Cortical Bone, Soft Tissue and PMMA. It was used the transmission method to obtain experimental attenuation coefficients to all materials. HVL for the materials were also calculated. Results show that PLA-based printing filaments mixed with metals (Al, BRASS and Cu) has higher attenuation than pure PLA. Comparing the experimental data with theoretical cross section of Soft Tissue, Cortical Bone and PMMA, it was possible to observe that with the increase of beam energy, ABS-based and other blends' attenuation behaviour agree with PMMA/Soft tissue. None of the studied materials showed agreement of attenuation with Cortical Bone. Some variations of PLA (SILK, Black and Bone) and some of the other blends of PETG and TPU showed good agreement with Soft Tissue/PMMA since about 30 keV and it can be concluded that these filaments can be used as substitute of PMMA for mimetizing soft tissue in 3D printed phantoms.

1. Introduction

3D printing is revolutionizing all the areas of knowledge, and with radiation dosimetry and quality assurance is no different. The first 3D printing technologies were created in the 80's (Hull, 1984; Crump, 1992) and initially were mainly used in industry. In the last 10 years, health and physics dawned the use to build a variety of phantoms, especially simulators of the human body, as a result of the great evolution occurred in machinery, materials and cost of the 3D printing technology.

Several 3D printers are commercially available and these equipments nowadays are worldwide spread and the costs for the acquisition and maintenance of this equipment are becoming smaller. Especially equipment based on Fusion Filament Fabrication (FFF), investigations on feasibility of 3D printing phantoms for medical and dosimetric applications are increasing (Santos et al., 2019; Kadoya et al., 2019) since the technique allows the possibility of mixing and varying between filaments and print configurations. The available literature on FFF technology (Robinson et al., 2016; Kamomae et al., 2017; Craft and Howell, 2017; O'Dell et al., 2017; Villani et al., 2020), applied to phantom prototyping mostly explore two of most common polymers in 3D printing: acrylonitrile butadiene styrene (ABS) and Polylactic Acid (PLA), although there are a significant number of different materials and blends commercially available that can be used to mimetize human soft tissue not already tested. Our recent studies identified the Hounsfield number behaviour in Computed Tomography (CT) imaging of commercial 3D printing filaments (Savi et al., 2020).

This paper aims to report the attenuation behaviour of several commercially available 3D printing filaments to be applied on development of 3D printed tissue equivalent phantoms with low cost. The attenuation was evaluated for standard X-ray beams from 29.7 keV to 46.5 keV of mean energy and experimental results are compared with NIST Database and ICRU 44 (Hubbell and Seltzer, 2004; White et al., 1989) theoretical data of radiation cross section for Cortical Bone, Soft Tissue and PMMA. The first two materials were chosen based on their prevalence in the human body and their importance on the development of a tissue equivalent phantom. PMMA was included as it is standard reference phantom material for soft tissue equivalence (White et al., 1989).

* Corresponding author. Instituto Federal de Santa Catarina – IFSC, Avenida Mauro Ramos, 950. Centro, Florianópolis, SC, 88020-300, Brazil.
E-mail address: matheus.savi@ifsc.edu.br (M. Savi).

https://doi.org/10.1016/j.radphyschem.2021.109365
Received 14 September 2020; Received in revised form 13 December 2020; Accepted 21 January 2021
Available online 4 February 2021
0969-806X/

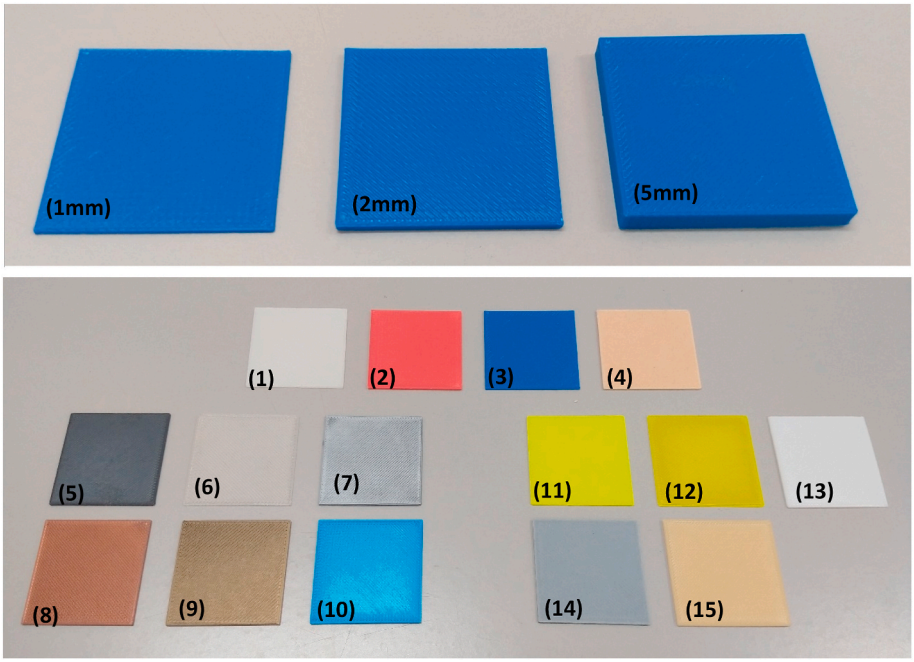

Fig. 1. 3D printed plates used in this study. Details of each printed plate is presented in Table 1 for each indicated sample number.

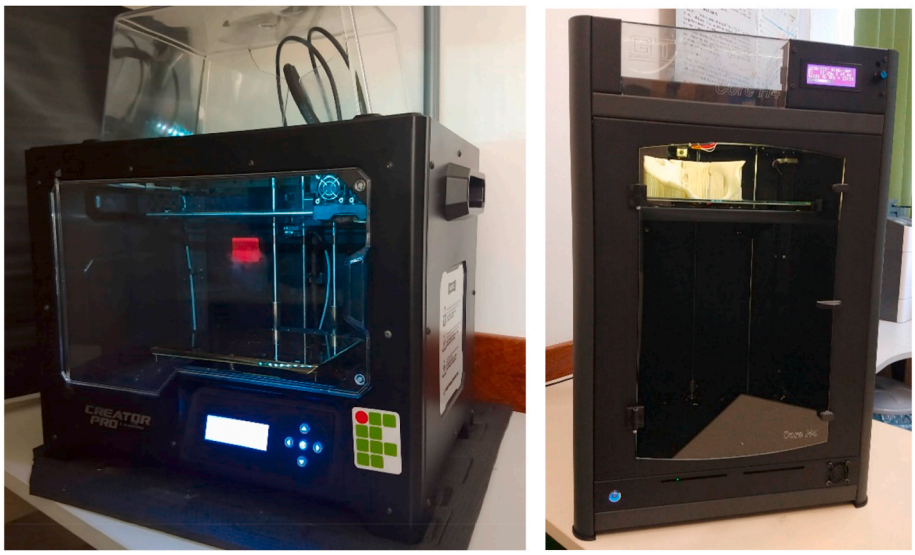

Fig. 2. 3D printers used in this study. (a) Flashforge Creator Pro 3D and (b) GTMax3D Core H4.

2. Material and methods

2.1. 3D printing materials and printing set-up

This study evaluates several 3D printing materials commercially available. Plates of each material were printed with dimensions of 40 × 40 mm^2 and varied thickness of 1, 2 and 5 mm (Fig. 1) in 100% rectilinear (+45°/-45°) infill in a Flashforge Creator Pro 3D and a GTMax3D Core H4 3D printers (Fig. 2) available at Radiation Protection Research Group of the Instituto Federal de Santa Catarina (IFSC). The details of the 3D printing filaments and printing protocols used can be found in Table 1.

2.2. Radiation beams

The IEC 61267 (1994) standard X-ray beams established at the Instrument Calibration Laboratory of Nuclear and Energy Research Institute (IPEN) were used to study the attenuation behaviour of the 3D printing filaments to photons, with energy range of diagnostic applications. The RQR standard beams were generated using the X-ray system Pantak/Seifert ISOVOLT 160. Specifications of the radiation beams can be found in Table 2.

2.3. Radiation detector

In order to obtain the values of transmitted radiation beams for the experimental measurements, a calibrated commercial radiation detection system RaySafe was used, with X2 R/F solid-state sensor connected.

2.4. Irradiation set-up and data analysis

The transmission method was used aiming to determine experi-

Table 1
Materials specifications and 3D printing set-up characteristics used in this work.

Nº	Material		Producer	Nominal Density (g. cm^{-3})	Experimental Density (Savi et al., 2020) ($g.cm^{-3}$)	Nozzle Temperature (ºC)	Heated Bed Temperature (ºC)	Print Speed (mm/s)
1	ABS-based	ABS	3DON	1.04	0.911(1)	225	100	66
3		Red ABS	FlashForge	NA	0.9375(9)	235	105	50
3		ABS+	UP3D	1.05	0.9919(7)	235	100	66
4		ABS WOOD	UP3D	NA	1.0763(7)	230	55	66
5	PLA-based	Black PLA	UP3D	1.25	1.1027(8)	190	60	91
6		PLA + Bone	UP3D	NA	1.131(5)	195	60	108
7		PLA + Al	UP3D	NA	0.987(1)	190	70	91
8		PLA + Cu	UP3D	NA	1.127(2)	220	105	33
9		PLA + Brass	UP3D	NA	1.197(1)	225	60	91
10		SILK	UP3D	NA	1.1837(8)	200	50	108
11	Other blends	HIPS	UP3D	1.04	0.926(6)	190	70	21
12		PETG	UP3D	1.25	1.057(2)	235	100	60
13		TPE	UP3D	NA	0.7940(9)	245	100	9
14		TPU	UP3D	NA	1079(3)	240	75	20
15		PVA	UP3D	1.19	1.050(3)	200	100	9

Table 2
Standard radiation beam qualities used in this study.

Beam Quality	Tube voltage	HVL	Additional Filtration	Mean photon energy
	(kVp)	(mmAl)	(mm)	(keV)
RQR 3	50	1.78	2.4Al	29.7
RQR 5	70	2.58	2.8Al	34.0
RQR 8	100	3.97	3.2Al	38.1
RQR 10	150	6.57	4.2Al	46.5

mentally the attenuation coefficients (μ) of the materials. A simple exponential attenuation should be expected as result of the strike of the beam in a detector after passing through absorbers of variable thickness. The interactions remove photons from the beam either by absorption or by scattering away from the detector and can be characterized by a fixed probability of occurrence per unit path length in the absorber. The sum of them is the probability per unit path length that the photon is removed (Knoll, 2010; Tsoulfanidis, 2010)

$$\mu = \tau + \sigma + \kappa \quad (1)$$

where τ is the absorption by photoelectric effect, σ Compton scattering and κ pair production.

The measurements were carried out with the 3D printed plates as beam absorbers, and they were positioned in front of the beam exit with thickness increasing from zero to 10 mm (details in Fig. 3). The values obtained in this procedure were analyzed using Origin® software. For each beam quality, an exponential fit was performed in order to obtain μ of the materials to each X-ray beam quality according to Eq. (2) (Knoll, 2010; Tsoulfanidis, 2010)

$$I_t = I_0 e^{-\mu t} \quad (2)$$

where I_0 is the initial beam intensity, and I is the beam intensity when some material of thickness t is placed between radiation source and detector. The use of the linear attenuation coefficient is limited by the fact that it varies with the density of the absorber, even though the absorber material is the same. The total mass attenuation coefficient (μ_m) is independent on the density of the absorber and is defined as Eq. 3

$$\mu_m = \frac{\mu}{\rho} \quad (3)$$

where ρ is the density of the absorber.

The transmission method considers the incident photons being monoenergetic (Knoll, 2010; Tsoulfanidis, 2010). Measurements in this study were performed using polyenergetic X-ray filtered beams, and this methodology is a great approximation to be used to theoretical data comparison (Villani et al., 2020). Once the linear attenuation

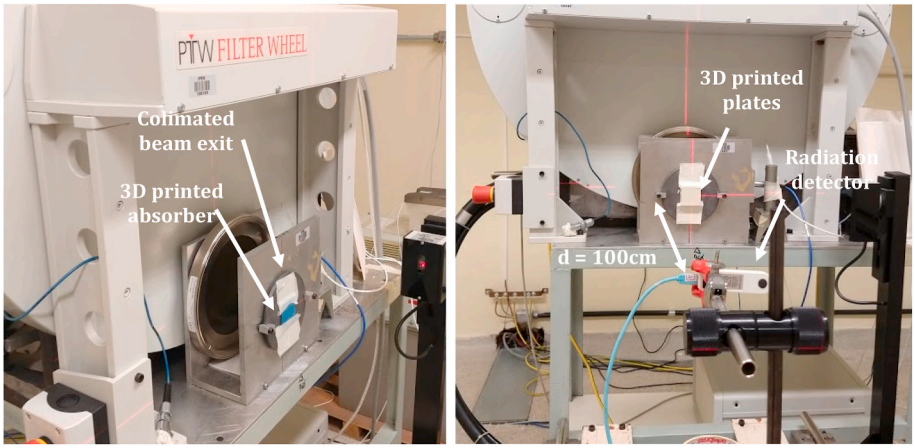

Fig. 3. Irradiation set-up for the transmission measurements on Pantak X-ray system in accordance with TRS 457 (IAEA, 2007) and IEC 61267 (IEC, 1994) guidelines for calibration. Source/beam exit – beam detection distances used were 100 cm. The attenuation 3D printed plates were positioned at the beam exit.

Table 3
Material constants and composition assumed for compounds and mixtures (Hubbell and Seltzer, 2004; White et al., 1989).

Material	Density (g.cm^{-3})	Component	Z	Fraction by weight
Cortical Bone	1.920	H	1	0.034000
		C	6	0.155000
		N	7	0.042000
		O	8	0.435000
		Na	11	0.001000
		Mg	12	0.002000
		P	15	0.103000
		S	16	0.003000
		Ca	20	0.225000
Soft Tissue	1.060	H	1	0.102000
		C	6	0.143000
		N	7	0.034000
		O	8	0.708000
		Na	11	0.002000
		P	15	0.003000
		S	16	0.003000
		Cl	17	0.002000
		K	19	0.003000
PMMA	1.190	H	1	0.080541
		C	6	0.599846
		O	8	0.319613

coefficients are calculated, the experimental values of the total mass attenuation and half-value layer (HVL) for the 3D printed phantoms can be calculated using Eq. (3) and Eq. (4) respectively

$$HVL = \frac{ln\,(2)}{\mu} \tag{4}$$

The experimental results of total mass attenuation were compared with theoretical data for Cortical Bone, Soft Tissue – human components of most interest when building a phantom – and PMMA, standard material for mimetizing soft tissue in a majority of dosimetry applications (White et al., 1989). NIST database and ICRU report 44 were used to obtain the composition of the mixtures (Table 3) and XCOM (NIST, 2020) to obtain the theoretical photon cross section, and results plotted alongside experimental data for comparison.

3. Results

3.1. Radiation transmission measurements

Using Eq. (2) to the data points from the radiation transmission of the printed materials to the standard X-ray beams, it is obtained the experimental results on linear attenuation coefficients (μ). Fig. 4A to D shows these results to the beam qualities measured, and respective values of μ presented in Table 4. One can observe that the values of linear attenuation are dependent on beam quality, expected as beams energy increase the attenuation decreases.

3.2. Half-value layer (HVL)

Using the attenuation coefficients (μ) of Table 4 and Eq. (3), the experimental values of HVL were calculated to the printing material to all X-ray beams studied. These results are presented in Table 5. As expected, the HVL values of the printing materials also increase as the mean photon energy of the beams increase.

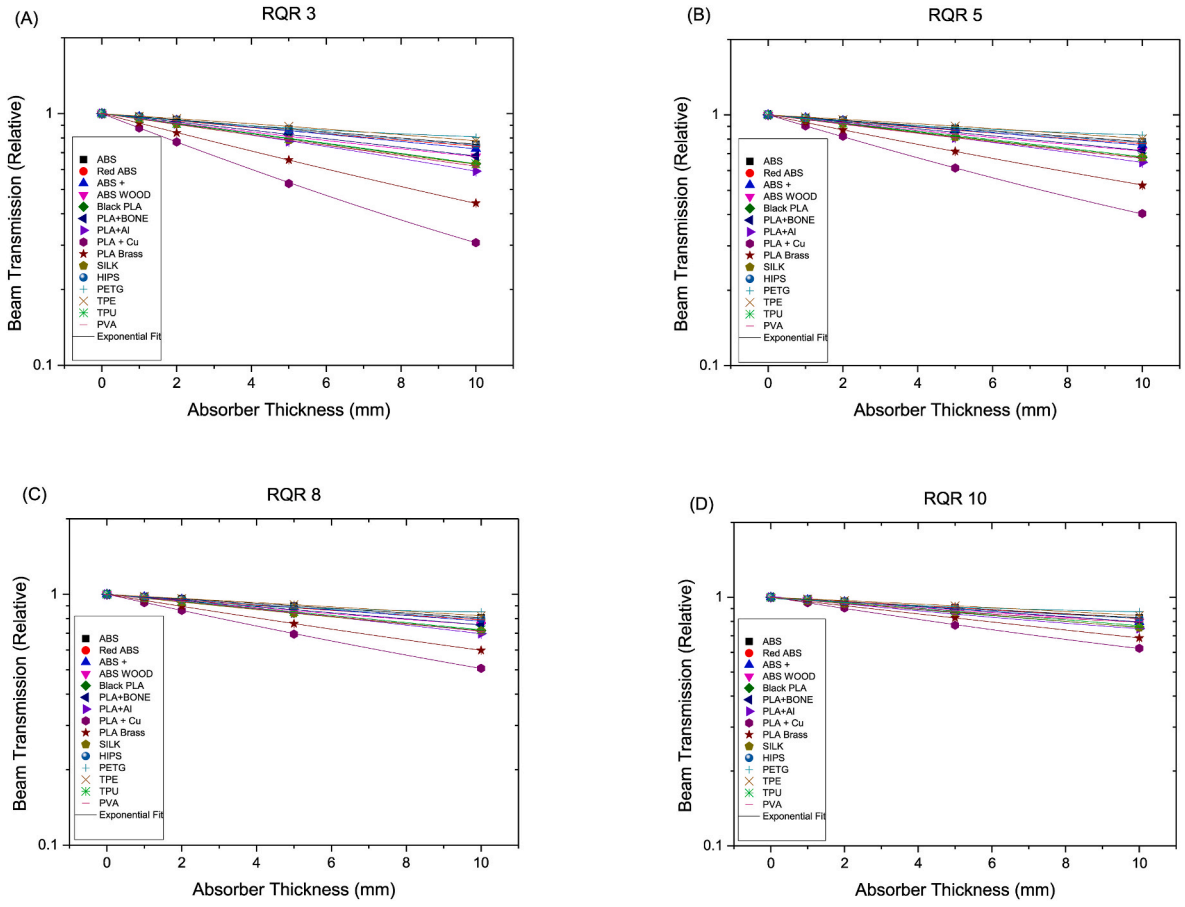

Fig. 4. Experimental data points and respective fitted curves for the 3D printing materials for (A) RQR 3; (B) RQR 5; (C) RQR 8 and (D) RQR 10 standard X-ray beams.

Table 4
Experimental linear attenuation coefficients obtained.

ABS-based	Beam Quality	ABS μ (cm^{-1})	Adjust R^2	Red ABS μ (cm^{-1})	Adjust R^2	ABS + μ (cm^{-1})	Adjust R^2	WOOD μ (cm^{-1})	Adjust R^2
	RQR3	0.285 ± 0.059	0.9997	0.305 ± 0.036	0.9982	0.320 ± 0.021	0.9998	0.392 ± 0.045	0.9980
	RQR5	0.247 ± 0.061	0.9999	0.262 ± 0.026	0.9988	0.279 ± 0.011	0.9992	0.329 ± 0.031	0.9990
	RQR8	0.218 ± 0.065	0.9999	0.235 ± 0.016	0.9992	0.250 ± 0.034	0.9999	0.283 ± 0.014	0.9990
	RQR10	0.193 ± 0.037	0.9999	0.201 ± 0.012	0.9999	0.230 ± 0.033	0.9999	0.235 ± 0.019	0.9989

PLA-based	Beam Quality	PLA BLACK μ (cm^{-1})	Adjust R^2	PLA + BONE μ (cm^{-1})	Adjust R^2	PLA + Al μ (cm^{-1})	Adjust R^2	PLA + Cu μ (cm^{-1})	Adjust R^2	PLA Brass μ (cm^{-1})	Adjust R^2	SILK μ (cm^{-1})	Adjust R^2
	RQR3	0.463 ± 0.048	0.9999	0.394 ± 0.013	0.9999	0.529 ± 0.029	0.9994	1.182 ± 0.016	0.9982	0.822 ± 0.014	0.9994	0.458 ± 0.051	0.9996
	RQR5	0.393 ± 0.057	0.9994	0.332 ± 0.031	0.9998	0.439 ± 0.054	0.9995	0.913 ± 0.043	0.9984	0.642 ± 0.037	0.9999	0.393 ± 0.005	0.9995
	RQR8	0.329 ± 0.024	0.9997	0.283 ± 0.021	0.9999	0.379 ± 0.013	0.9993	0.679 ± 0.049	0.9985	0.529 ± 0.013	0.9996	0.328 ± 0.015	0.9999
	RQR10	0.282 ± 0.041	0.9999	0.239 ± 0.026	0.9998	0.293 ± 0.015	0.9978	0.479 ± 0.012	0.9977	0.439 ± 0.046	0.9996	0.277 ± 0.009	0.9996

Other blends	Beam Quality	HIPS μ (cm^{-1})	Adjust R^2	PETG μ (cm^{-1})	Adjust R^2	TPE μ (cm^{-1})	Adjust R^2	TPU μ (cm^{-1})	Adjust R^2	PVA μ (cm^{-1})	Adjust R^2
	RQR3	0.289 ± 0.013	0.9995	0.449 ± 0.045	1.0	0.250 ± 0.039	0.9987	0.458 ± 0.018	0.9999	0.485 ± 0.054	0.9999
	RQR5	0.253 ± 0.012	0.9995	0.375 ± 0.031	1.0	0.221 ± 0.044	0.9989	0.379 ± 0.018	0.9999	0.404 ± 0.030	0.9991
	RQR8	0.218 ± 0.032	0.9992	0.327 ± 0.014	0.9998	0.213 ± 0.049	0.9992	0.327 ± 0.025	0.9999	0.345 ± 0.041	0.9998
	RQR10	0.197 ± 0.031	0.9992	0.271 ± 0.019	1.0	0.179 ± 0.019	0.9988	0.268 ± 0.047	0.9997	0.229 ± 0.013	0.99822

Table 5
Experimental HVL calculated for the 3D printing materials.

ABS-based	Beam Quality	ABS HVL (cm)	Red ABS HVL (cm)	ABS + HVL (cm)	WOOD HVL (cm)
	RQR3	2.430 ± 0.086	2.276 ± 0.053	2.162 ± 0.031	1.769 ± 0.065
	RQR5	2.777 ± 0.087	2.644 ± 0.038	2.485 ± 0.015	2.107 ± 0.044
	RQR8	3.182 ± 0.094	2.952 ± 0.023	2.766 ± 0.044	2.445 ± 0.020
	RQR10	3.599 ± 0.053	3.442 ± 0.018	3.014 ± 0.048	2.955 ± 0.027

PLA-based	Beam Quality	Black PLA HVL (cm)	PLA + BONE HVL (cm)	PLA + Al HVL (cm)	PLA + Cu HVL (cm)	PLA Brass HVL (cm)	SILK HVL (cm)
	RQR3	1.496 ± 0.007	1.759 ± 0.018	1.309 ± 0.042	0.586 ± 0.023	0.843 ± 0.012	1.513 ± 0.012
	RQR5	1.763 ± 0.008	2.087 ± 0.044	1.577 ± 0.078	0.759 ± 0.062	1.079 ± 0.054	1.765 ± 0.020
	RQR8	2.106 ± 0.004	2.452 ± 0.030	1.826 ± 0.019	1.020 ± 0.072	1.309 ± 0.019	2.112 ± 0.021
	RQR10	2.460 ± 0.006	2.903 ± 0.038	2.364 ± 0.021	1.447 ± 0.018	1.580 ± 0.067	2.502 ± 0.013

Other blends	Beam Quality	HIPS HVL (cm)	PETG HVL (cm)	TPE HVL (cm)	TPU HVL (cm)	PVA HVL (cm)
	RQR3	2.402 ± 0.019	1.544 ± 0.065	2.765 ± 0.057	1.514 ± 0.026	1.430 ± 0.077
	RQR5	2.736 ± 0.019	1.851 ± 0.044	3.143 ± 0.064	1.828 ± 0.027	1.714 ± 0.043
	RQR8	3.188 ± 0.046	2.117 ± 0.020	3.242 ± 0.072	2.119 ± 0.035	2.009 ± 0.059
	RQR10	3.515 ± 0.045	2.562 ± 0.027	4.058 ± 0.029	2.585 ± 0.067	3.023 ± 0.019

3.3. Total mass attenuation (μ_m)

Derived from linear attenuation coefficients and measured densities, the total mass attenuation of the printing materials was obtained and compared with theoretical data of Cortical Bones, Soft Tissue and PMMA. Fig. 5 show the theoretical and experimental results plotted along each other. Analysing the results, it is possible to observe that the agreement between PMMA and Soft Tissue behaviour for the printing materials improves with the increase of X-ray beam energy. The PLA-based materials mixed with metals, such as PLA + Al, PLA + BRASS and PLA + Cu has higher attenuation properties among all 3D printing materials evaluated, but without satisfactory attenuation agreement with Cortical Bone.

4. Discussions

Nowadays it is crucial for the areas of dosimetry and medical physics to incorporate technologies into clinical routine aiming to improve quality assurance to treatments and equipment calibration. The evaluation of attenuation behaviour of 3D printing materials opens a wide

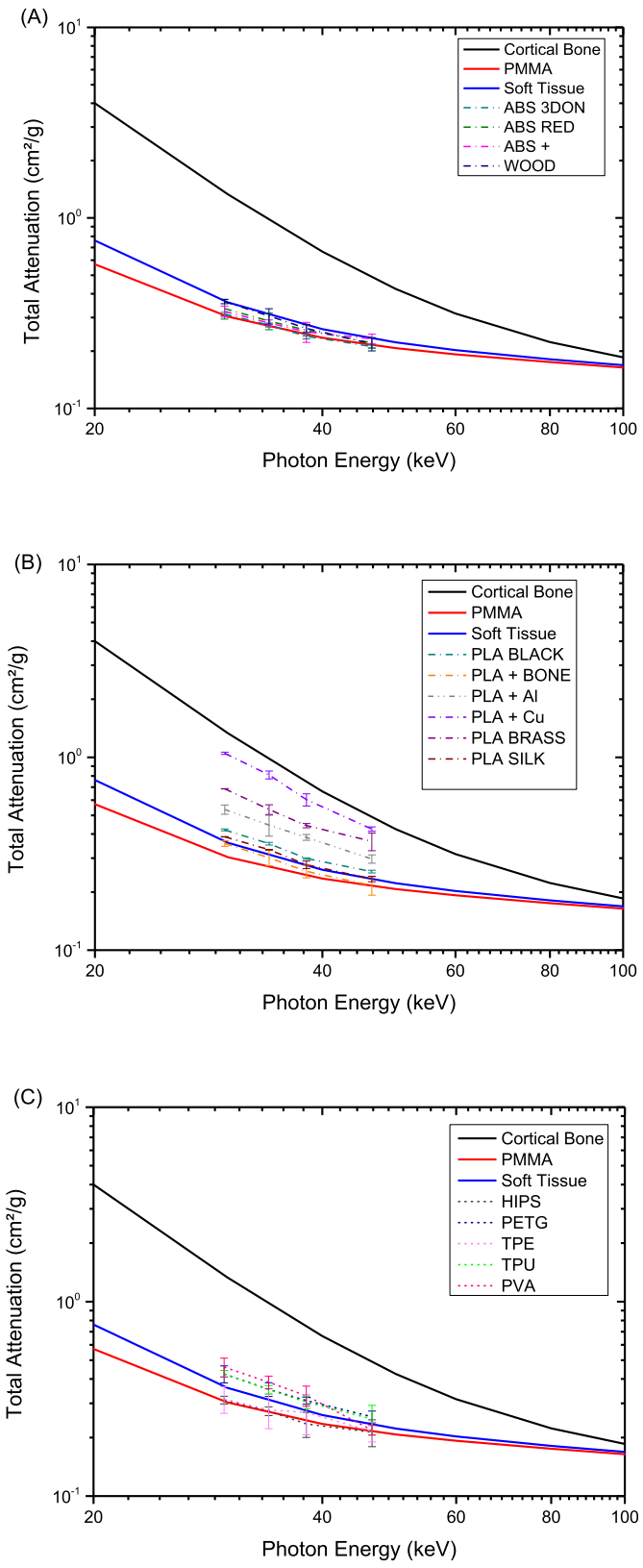

Fig. 5. Experimental total mass attenuation behaviour of 3D printing materials and theoretical data. (a) ABS-based filaments (b) PLA-based filaments (c) Other blends filaments.

range of possibilities for construction of tissue equivalent and, since the technology already are widely available, low cost 3D printed phantoms with complex geometries.

The X-ray qualities used varied from 29.7 keV, where photoelectric effect prevails, to 45.6 keV, slightly higher energy beams where there is some increase in Compton scattering. Thus, it is possible to observe that differences on μ for each material relates on beam energy and the transmission method used to our measurements sum Photoelectric and Compton interactions. Analysing the results one can observe that all the ABS-based materials presented statistically equivalent linear attenuation (within 1σ) for the RQR 3, RQR5 and RQR8 beam qualities. PLA-based filaments with "heavy" metals (Cu, Al and BRASS) presented higher attenuation properties throughout all the energy range studied, resulting in thinner HLV thicknesses as showed in Table 5.

PLA filaments without heavy additives (SILK, Black and Bone) and other blend filaments (PETG and TPU) show narrow equivalence (statistically equivalent within 1σ) with Soft Tissue and PMMA theoretical data, especially for RQR 8 and RQR10 qualities. The radiation beams used in this study are likely to harden by increasing the thickness of the absorbers during measurements, since the X-rays produced on Pantak/Seifert ISOVOLT 160 are not monoenergetic, nevertheless, considering the experimental uncertainties, our findings using this set-up are consistent with the theoretical data.

The attenuation properties of the materials used for FFF 3D printing may change according with the used printing configurations, e.g. by varying the infill percentages of the printed phantoms (Villani et al., 2020). This change affects the Computed Tomography (CT) imaging of the materials as well, as documented by Andrade et al. (2019), Savi et al. (2020). Therefore, even PLA-based filaments with metals could mimic some variations soft tissue if applying these changes in printing configuration but none of the 3D printing materials in this study presented equivalence in attenuation with Cortical Bone. These findings show that in order to be able to develop tissue-equivalent simulators using 3D printing technology by FFF, there is a gap on research and development of compatible printing filaments to this end.

5. Conclusions

This paper reports the attenuation behaviour of commercial 3D printing commercial filaments over standard X-ray beams. Experimental results show that variations of PLA (SILK, Black and Bone) and polymer blends as PETG and TPU presented good agreement with Soft Tissue/PMMA from about 30 keV and it can be concluded that all these filaments can be used as substitute of PMMA for mimetizing soft tissue in 3D printed phantoms. ABS-based filaments studied can as well be used to these applications but the energy range of radiation must be concerned. New commercial 3D printing filaments have yet be developed as suitable substitute for Cortical Bone attenuation characteristics.

Authors statement

Savi, M: Conceptualization, Methodology, Validation, Investigation, Resources, Writing - Original Draft, Project administration, Funding acquisition,

Andrade, M.A.B: Investigation, Resources, Writing - Original Draft, Writing - Review & Editing

Villani, D.: Investigation, Writing - Original Draft, Writing - Review & Editing.

Rodrigues Jr.: Methodology, Writing - Review & Editing.

Potiens, M.P.A: Methodology Writing - Review & Editing, Supervision, Funding acquisition

Declaration of competing interest

The authors declare that they have no known competing financial interests or personal relationships that could have appeared to influence

the work reported in this paper.

Acknowledgments

The authors would like to thank PROPPI/IFSC, CAPES, FAPESP (PROJECT 2017/50332-0) and CNPq (PROJECT 312131/2016-0 and process number 42098/2017-5) for the financial support.

References

Andrade, M.A.B., Alves, C.O., Fin, A.P.C., Soares, F.A.P., Savi, M., Potiens, M.P.A., 2019. Visual impact of infill percentages for 3D printed radiologic simulators. International Joint Conference Radio.

Craft, D.F., Howell, R.M., 2017. Preparation and fabrication of a full-scale, sagittal-sliced, 3D-printed, patient-specific radiotherapy phantom. J. Appl. Clin. Med. Phys. 18, 285–292.

Crump, S. Scott, June 1992. Apparatus and method for creating three-dimensional objects. US Patent 5121329.

Hubbell, J.H., Seltzer, S.M., 2004. X-ray mass attenuation coefficients. NIST Standard Reference Database 126. https://doi.org/10.18434/T4D01F.

Hull, C.W., August 1984. Apparatus for Production of Three-Dimensional Objects by Stereolithography. US Patent 4575330A.

IEC 61267, 1994. INTERNATIONAL ELECTROTECHNICAL COMMISSION. Medical Diagnostic X-Ray Equipment-Radiation Conditions for Use in the Determination of Characteristics.

Kadoya, N., Abe, K., Nemoto, H., et al., 2019. Evaluation of a 3D-printed heterogeneous anthropomorphic head and neck phantom for patient-specific quality assurance in intensity-modulated radiation therapy. Radiol Phys Technol 12, 351. https://doi.org/10.1007/s12194-019-00527-5.

Kamomae, T., Shimizu, H., Nakaya, T., et al., 2017. Three-dimensional printer- generated patient-specific phantom for artificial in vivo dosimetry in radiotherapy quality assurance. Phys. Med. 44, 205–211.

Knoll, Glenn F., 2010. Radiation Detection and Measurement. John Wiley & Sons.

O'Dell, W.G., Gormaley, A.K., Prida, D.A., 2017. Validation of the Gatortail method for accurate sizing of pulmonary vessels from 3D medical images. Med. Phys. 44, 6314–6328.

Robinson, A.P., Tipping, J., Cullen, D.M., et al., 2016. Organ-specific SPECT activity calibration using 3D printed phantoms for molecular radiotherapy dosimetry. EJNMMI Phys 3, 12. https://doi.org/10.1186/s40658-016-0148-1.

Santos, J.C., Almeida, C.D., Iwahara, A., Peixoto, J.E., 2019. Characterization and applicability of low-density materials for making 3D physical anthropomorphic breast phantoms. Radiat. Phys. Chem. 164 https://doi.org/10.1016/j.radphyschem.2019.108361.

Savi, M., Andrade, M.A., Potiens, M.P., 2020. Commercial filament testing for use in 3D printed phantoms. Radiat. Phys. Chem. 108906. https://doi.org/10.1016/j.radphyschem.2020.108906.

TRS 457, 2007. INTERNATIONAL ATOMIC ENERGY AGENCY. Dosimetry in Diagnostic Radiology: an International Code of Practice. IAEA, Vienna. IAEA technical report series 457.

Tsoulfanidis, Nicholas, 2010. Measurement and Detection of Radiation. CRC press.

Villani, D., Rodrigues Jr., O., Campos, L.L., 2020. Dosimetric characterization of 3D printed phantoms at different infill percentages for diagnostic X-ray energy range. Radiat. Phys. Chem. 172, 108728. https://doi.org/10.1016/j.radphyschem.2020.108728.

White, D.R., Booz, J., Griffith, R.V., Spokas, J.J., Wilson, I.J., 1989. Tissue substitutes in radiation dosimetry and measurement. In: ICRU Report 44, International Commission on Radiation Units and Measurements, USA. https://doi.org/10.1093/jicru/os23.1.Report44.

XCOM NIST. Photon cross-sections database. Available in: https://physics.nist.gov/PhysRefData/Xcom/html/xcom1.html.